Available online at www.sciencedirect.com
ScienceDirect
Trans. Nonferrous Met. Soc. China 32(2022) 1242−1252
Transactions of Nonferrous Metals Society of China
www.tnmsc.cn

# Relaxor ferroelectric and dielectric properties of $(1-x)Ba(Zr_{0.1}Ti_{0.9})O_3-xBa(Mg_{1/3}Ta_{2/3})O_3$ ceramics

Jesse Nii Okai AMU-DARKO[1,2], Chen ZHANG[1], Shahid HUSSAIN[2],
Samuel Leumas OTOO[3], Michael Freduah AGYEMANG[4]

1. School of Materials Science and Engineering,
Jiangsu University of Science and Technology, Zhenjiang 212100, China;
2. School of Materials Science and Engineering, Jiangsu University, Zhenjiang 212013, China;
3. School of Materials Science and Engineering, Wuhan University of Technology, Wuhan 430070, China;
4. Department of Materials and Earth Sciences,
Technische Universität Darmstadt Alarich-Weiss-Straße 2, 64287 Darmstadt, Germany

Received 23 March 2021; accepted 24 September 2021

**Abstract:** The environmentally-friendly $(1-x)Ba(Zr_{0.1}Ti_{0.9})O_3-xBa(Mg_{1/3}Ta_{2/3})O_3$ ($x$=0, 0.02, 0.04, 0.06, 0.08) relaxor ferroelectric ceramics were prepared by the conventional solid-state method and sintered in air at 1400 °C for 2 h. SEM and XRD analyses were utilized to study the surface morphologies and the crystalline structures, respectively. The effects of $Ba(Mg_{1/3}Ta_{2/3})O_3$ on the phase transformation, dielectric and ferroelectric properties of $Ba(Zr_{0.1}Ti_{0.9})O_3$ ceramics were also investigated. It is found that the average grain size of $(1-x)Ba(Zr_{0.1}Ti_{0.9})O_3-xBa(Mg_{1/3}Ta_{2/3})O_3$ (BZT−BMT) perovskite single-phase ceramics decreases as the content of $Ba(Mg_{1/3}Ta_{2/3})O_3$ (BMT) increases. The relaxor ferroelectric behavior with diffuse phase transition and well-defined frequency dispersion of dielectric maximum temperature is found for the ceramic with increasing $x$ values. 0.98BZT−0.02BMT ceramic shows very good dielectric properties with the relative permittivity and the dielectric loss, measured at 100 kHz as 6034 and 0.01399 respectively at room temperature. Both remnant polarization and coercive field decreased with increasing BMT content, indicating a transition from the ferroelectric phase to the paraelectric phase at room temperature.
**Key words:** barium zirconate titanate; perovskite; relaxor ferroelectrics; dielectric properties; phase transition

## 1 Introduction

Electronic devices and equipment have taken center stage and play major roles in daily life activities over the last few decades. According to SEBASTIAN et al [1], the income generated from interconnected devices for cellular network operators alone in the sectors of the automotive, health sector, and consumer electronics should be about US$1.3 trillion by 2020. In view of this, there is a need to meet the specifications of future systems, new designs and improved or new dielectric components are required. Barium titanate ($BaTiO_3$) based ceramics are the first simple metal oxide compounds in which ferroelectric behavior was observed. After 60 years of its discovery, barium titanate still rates as the base material of choice for ceramic dielectrics due to its good characteristic properties [2,3]. Its high dielectric constant and low loss make it the main reason why barium titanate is an excellent option for industrial applications, such as capacitors [3], multilayer capacitors (MLCs) [4], and energy storage devices [5] with high efficiencies. Doped or composite barium titanate has wide application in

**Corresponding author:** Chen ZHANG, Tel: +86-511-84401184, Fax: +86-511-84407381, E-mail: czhang1981@hotmail.com
DOI: 10.1016/S1003-6326(22)65870-9

piezoelectric devices, semiconductors, sensors [6], ultrasonic transducers [7], and has outrightly become one of the most important ferroelectric ceramics [8,9]. A nonlinear dielectric behavior with three distinct peaks is observed for pure $BaTiO_3$ as a result of the phase transition from rhombohedral to orthorhombic at −90 °C, orthorhombic to tetragonal at 0 °C, and tetragonal to cubic at 120 °C [10]. Modification of barium titanate shifts its Curie peaks to lower temperatures and varies the temperature coefficient of capacitance for use in capacitor application. This is usually achieved by substituting small-sized divalent ions for barium and bigger tetravalent ions for titanium.

There have been tremendous efforts devoted in the last decade to modify similar competitive lead-free ceramics, such as $CaTiO_3$ (CTO) [11,12], $(K,Na)NbO_3$ (KNN) [13,14], $(Bi_{1/2}Na_{1/2})TiO_3$(BNT) [15], and bismuth layer-structured ferroelectrics (BLSF) [16,17].

Barium zirconium titanate (BZT) has a typical perovskite structure with the chemical composition as $ABO_3$ [18−20]. The *A*-site cations ($Ba^{2+}$) occupy the corners of the unit cell and the *B*-site cations ($Zr^{4+}/Ti^{4+}$) reside in the body center, whilst six oxygen anions ($O^{2-}$) are in the center of each face of the unit cell structure.

The behavior of the $BaZr_xTi_{(1-x)}O_3$ ceramics is reported to be a normal ferroelectric at $0<x<0.10$, a diffuse phase transition at $0.10<x<0.20$, and non-ferroelectric character at $x>0.20$ [21,22]. BZT based ceramics have been studied because of their relaxor properties which are largely caused by the site disorder charge of the perovskite structure due to the substitution of cations with a different valence [23,24].

X-ray diffraction studies on the lead-free $0.50Ba_{0.9}Ca_{0.1}TiO_3$−$0.50BaTi_{(1-x)}Zr_xO_3$ (BCT−BZT) ceramics show the phase transformation from orthorhombic to rhombohedral symmetry with increasing zirconium content with the dynamic phase transition observed at $x$=0.10 [25]. KANTHA et al [26] studied the electrical properties of the $(1-x)Bi_{0.4871}Na_{0.4871}La_{0.0172}TiO_3$−$BaZr_{0.05}Ti_{0.95}O_3$ (BNLT−BZT) system. The scanning electron microscopy images showed rectangular-shaped grains along with irregular grains that confirm a significant change in shape in the BNLT−BZT ceramics by the amount of BZT added. The microstructural analysis further revealed that BZT additions decreased the grain size from ~7.4 μm for the pure BNLT sample to ~1.6 μm for the highest doping content. The dielectric constants were enhanced with increasing BZT content with the highest recorded value being 4400. Evidence of phase transition and broadened dielectric−temperature curves, indicated that relaxor behavior of the ceramics was also observed. By using similar solid-state methods, ZHONG et al [27] also reported the dielectric properties and relaxor ferroelectric behavior of $(1-y)Ba(Zr_{0.1}Ti_{0.9})O_3$−$yBa(Zn_{1/3}Nb_{2/3})O_3$ ceramics ($y$=0−0.05). The permittivity maximum ($\varepsilon_{r,max}$) was observed to be subdued from 8948 to 1611 at a test frequency of 1 kHz with increasing $y$. The dielectric maximum temperature ($T_m$) decreased from 93 to −89 °C at 1 kHz as $y$ increased ($y$=0−0.05).

The present work reports the results of a dielectric study aimed at investigating the relaxor-like properties in the $(1-x)Ba(Zr_{0.1}Ti_{0.9})O_3$−$xBa(Mg_{1/3}Ta_{2/3})O_3$ ceramics prepared by the conventional solid-state method. It also unravels that the $Ba(Mg_{1/3}Ta_{2/3})O_3$ has apparent effects on the microstructure, dielectric and ferroelectric properties of $Ba(Zr_{0.1}Ti_{0.9})O_3$ ceramics for capacitor application.

## 2 Experimental

The $(1-x)Ba(Zr_{0.1}Ti_{0.9})O_3$−$xBa(Mg_{1/3}Ta_{2/3})O_3$ (BZT−BMT) ceramic system was prepared with $x$ (0, 0.02, 0.04, 0.06 and 0.08) having denotations shown in Table 1. The chemicals used in the preparation process were $BaCO_3$ (99%), $ZrO_2$ (99%), $TiO_2$ (99%), MgO (99%), and $Ta_2O_5$ (99%), obtained from Sinopharm Chemical Reagent Co., Ltd., without any further purification. Solid-state

**Table 1** Compositions of $(1-x)Ba(Zr_{0.1}Ti_{0.9})O_3$−$xBa(Mg_{1/3}Ta_{2/3})O_3$ ceramics

| $x$ | Denotation | Resultant formula |
|---|---|---|
| 0 | BMT0 | $Ba(Zr_{0.1}Ti_{0.9})O_3$ |
| 0.02 | BMT1 | $0.98Ba(Zr_{0.1}Ti_{0.9})O_3$−$0.02Ba(Mg_{1/3}Ta_{2/3})O_3$ |
| 0.04 | BMT2 | $0.96Ba(Zr_{0.1}Ti_{0.9})O_3$−$0.04Ba(Mg_{1/3}Ta_{2/3})O_3$ |
| 0.06 | BMT3 | $0.94Ba(Zr_{0.1}Ti_{0.9})O_3$−$0.06Ba(Mg_{1/3}Ta_{2/3})O_3$ |
| 0.08 | BMT4 | $0.92Ba(Zr_{0.1}Ti_{0.9})O_3$−$0.08Ba(Mg_{1/3}Ta_{2/3})O_3$ |

synthesis method was adopted for the production of the powder for samples.

The powders were mixed and ball-milled in distilled water for 24 h. The obtained mixtures were dried and then calcined in air at 1080 °C for 2 h. The obtained dry powders were ground with the addition of 5 wt.% polyvinyl alcohol (PVA) as a binder. The whitish powders obtained were pressed under 250 MPa into disks of diameter ~10 mm and sintered in air at 1400 °C for 2 h. To measure the electrical properties, the samples were coated with BQ−5311 silver paste as electrodes on both sides of the surface and then fired at 800 °C for 10 min.

The phase purity and crystalline structures of the sintered ceramic samples were confirmed by XRD (Rigaku D/max 2500v/pc) with Cu $K_\alpha$ radiation at the step of 2 (°)/min while the microstructural evaluation was done with the scanning electron microscope (JSM−6480 ESEM). The average grain sizes were further measured with the aid of the Nano Measurer software for Windows. The dielectric properties of the various samples were measured with TZDM−200−300C automatic electric parameter measuring system at 10, 100, 250, and 500 kHz at the temperatures of −180 to 120 °C. The hysteresis loops for the study of the ferroelectric behaviors were obtained by utilizing the Radiant Precision Premier II ferroelectric tester.

## 3 Results and discussion

### 3.1 Crystal structure

Figure 1(a) shows the room temperature XRD patterns of $(1-x)Ba(Zr_{0.1}Ti_{0.9})O_3-xBa(Mg_{1/3}Ta_{2/3})O_3$ ($x$=0, 0.02, 0.04, 0.06, 0.08). After comparing with the standard PDF diffraction card (PDF No. 31−0174), the occurrence of a perovskite phase structure is observed for all. The samples have no obvious impurity phase, but superlattice reflection peaks are detected for higher $Ba(Mg_{1/3}Ta_{2/3})O_3$ contents. This bespeaks the replacement of the ions at the *B*-sites resulting in the formation of solid solutions [28,29]. The noticeable phases for these ceramics are cubic (space group *Pm*3*m*) except for BMT3 and BMT4. The splitting of (200), (211) and (220) peaks is apparent for BMT4 and is a depiction of a pseudo-cubic phase (Fig. 1(b)). Hence, it is worth noting that the point of transition of the structure is just about $x$=0.06.

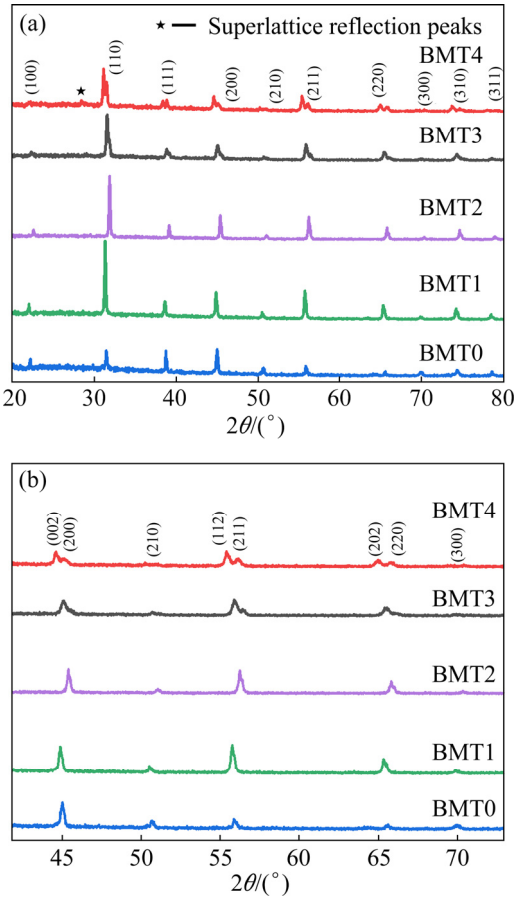


**Fig. 1** XRD patterns of BZT−BMT ceramics: (a) 2$\theta$= 20°−80°; (b) 2$\theta$=43°−73°

### 3.2 Microstructure

Figures 2(a)−(d) reveal the SEM images of BZT−BMT samples sintered at 1400 °C with $x$=0, 0.02, 0.06 and 0.08, respectively. The samples exhibited dense microstructure and clear grain boundaries with a bimodal grain size distribution, consisting of both faceted and polyhedral-shaped grains. The grain sizes decrease massively with the initial addition of BMT from 63.73 to 20.12 μm in BMT0 and BMT1 respectively, as seen in Table 2. It implies that the $Ta^{5+}$ (0.78 Å) and $Mg^{2+}$ (0.86 Å) substitution at the *B*-sites has a strong effect on the grain size, as a result of their relatively big ion radius which suppresses the grain growth. The Sample BMT4 (Fig. 2(d)) has some pores on its surface, which may be caused by the slightly higher dosage of PVA during the granulation process.

### 3.3 Dielectric properties

The room temperature dielectric constant ($\varepsilon_{r,RT}$) and dielectric loss (tan $\delta_{RT}$) at 100 kHz are listed in Table 3. It can be seen that, as the content of BMT

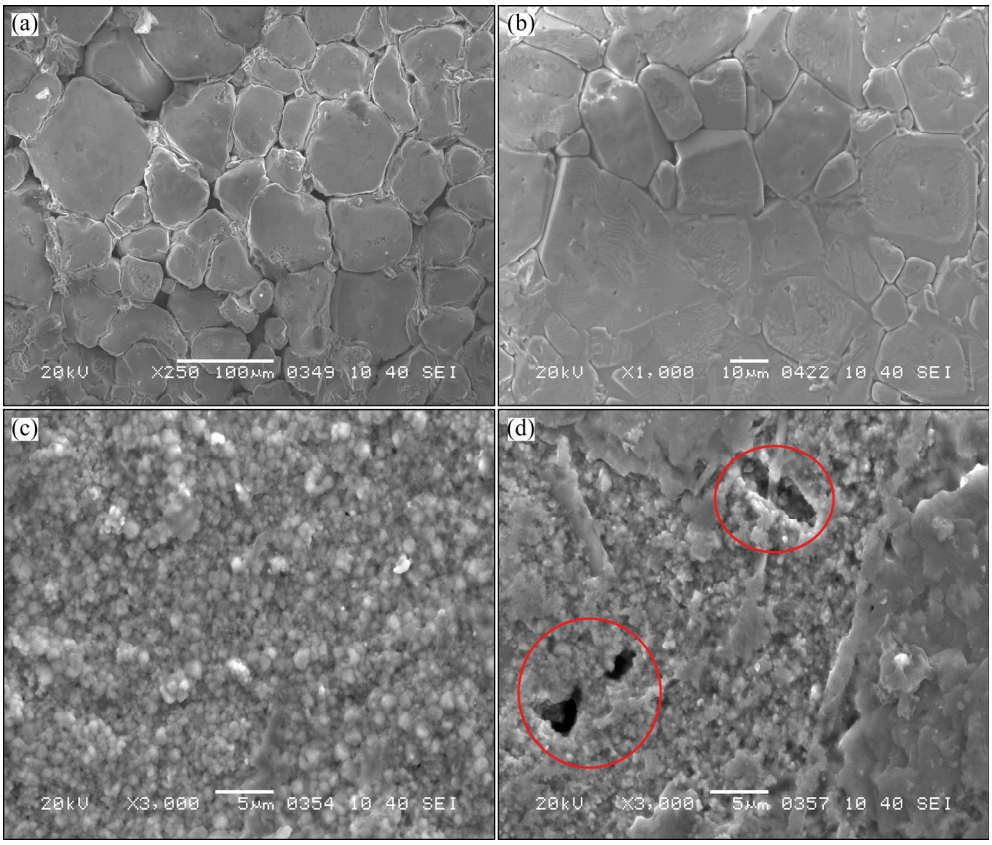


**Fig. 2** SEM images of BZT−BMT ceramics: (a) BMT0; (b) BMT1; (c) BMT3; (d) BMT4

**Table 2** Average grain sizes of BZT−BMT ceramics at 1400 °C (μm)

| BMT0 | BMT1 | BMT3 | BMT4 |
|---|---|---|---|
| 63.73 | 20.12 | 1.13 | 0.62 |

increases, the $\varepsilon_{r,RT}$ shows an increasing trend and then decreases. The room temperature dielectric constant of the BMT1 ceramic sample reached a maximum of 6034 and the loss was 0.01399. The decrease in the relative permittivity (when $x$ higher than 0.02) is caused by a decrease in the overall polarization of the ceramic samples due to the replacement reaction of zirconium and titanium ions in perovskite lattice. The tan $\delta_{RT}$ shows a minimum of 0.00552 for Sample BMT3. Further increasing the content of BMT causes a suppression of the $\varepsilon_{r,RT}$ which falls below 1000, at the same time maintaining a relatively low dielectric loss. For this reason, it can be said that the content of BMT has a significant effect on the room temperature dielectric constant and dielectric loss. And the proper content of BMT ($x$≈0.04) is beneficial to obtaining suitable BZT−BMT ceramic capacitors with higher

**Table 3** Dielectric properties of BZT−BMT ceramics at room temperature

| Sample | $\varepsilon_{r,RT}$ | tan $\delta_{RT}$ |
|---|---|---|
| BMT0 | 1909 | 0.01137 |
| BMT1 | 6034 | 0.01399 |
| BMT2 | 2996 | 0.00878 |
| BMT3 | 977 | 0.00552 |
| BMT4 | 644 | 0.00784 |

$\varepsilon_{r,RT}$ (≈3000) and lower tan $\delta_{RT}$ (<$9\times10^{-3}$). It is clear that the performance of BMT4 does not meet the product requirement of the ceramic capacitor due to the extremely low $\varepsilon_{r,RT}$, but is normal for application in all sample devices for mobile communication systems such as dielectric resonators and oscillators [30].

The temperature dependence of the relative permittivity and the dielectric loss for the $(1-x)Ba(Zr_{0.1}Ti_{0.9})O_3-xBa(Mg_{1/3}Ta_{2/3})O_3$ ceramics at 10, 100, 250, and 500 kHz are reported in Fig. 3. With the increase of the BMT content, the $\varepsilon_r-T$ curves are more broadened and the temperature

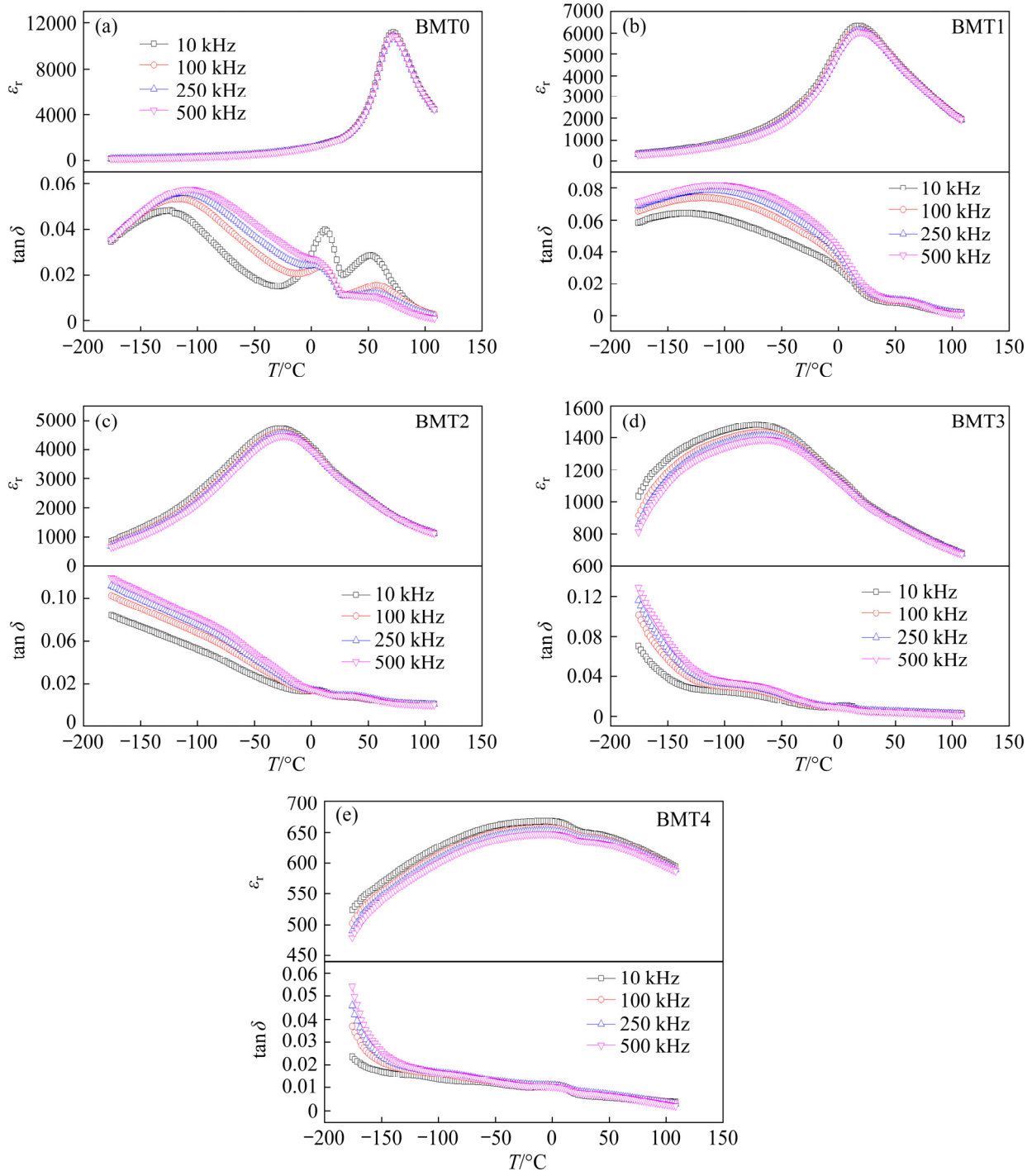


**Fig. 3** $\varepsilon_r$−$T$ and tan $\delta$−$T$ curves of BZT−BMT ceramics at multiple frequencies

corresponding to the dielectric maximum ($T_m$) moves to a lower temperature. The shift of the $T_m$ to lower temperatures is attributed to the weakening of the spontaneous polarization caused by the substitution of host ions. The resultant of the *B*-site substitution creates a local deformation of the perovskite unit cells, which also accounts for the reduction of the ferroelectric-paraelectric phase transition temperature [31,32]. In addition, the dielectric losses showed a decrease for every sample at high temperatures due to the low loss of the paraelectric phase. Moreover, loss peaks shifted gradually to lower temperatures even beyond the measured temperature.

Furthermore, as the content of BMT increases, the dielectric constant frequency dependence of the samples becomes more and more obvious, especially when $T<T_m$. In other words, the

frequency dispersion that is a major characteristic of relaxor ferroelectrics is clearly observed in BMT2, BMT3, and BMT4. Table 4 depicts how the test frequency affected the $T_m$ and the maximum dielectric constant ($\varepsilon_{r,max}$) of BMT2. The $T_m$ for the frequencies of 10, 100, 250 and 500 kHz was −26.4, −25.1, −22.8 and −21.2 °C, respectively. Table 5 also shows similar properties for Sample BMT3. In this case, the $T_m$ for 10, 100, 250 and 500 kHz was −70.8, −64.5, −60.9 and −58.8 °C, respectively. The frequency dispersion of $T_m$ for BMT3, by contrast, is stronger than that for BMT2, indicating an enhanced dielectric frequency dispersion characteristic of BZT−BMT ceramics with increasing BMT content.

**Table 4** Frequency dispersion of BMT2

| Frequency/kHz | $T_m$/°C | $\varepsilon_{r,max}$ |
|---|---|---|
| 10 | −26.4 | 4703 |
| 100 | −25.1 | 4568 |
| 250 | −22.8 | 4505 |
| 500 | −21.2 | 4457 |

**Table 5** Frequency dispersion of BMT3

| Frequency/kHz | $T_m$/°C | $\varepsilon_{r,max}$ |
|---|---|---|
| 10 | −70.8 | 1480 |
| 100 | −64.5 | 1429 |
| 250 | −60.9 | 1406 |
| 500 | −58.8 | 1385 |

Figure 4 shows the $\varepsilon_r$−$T$ and tan $\delta$−$T$ curves of BZT−BMT ceramics with different BMT contents at 100 kHz. It shows the apparent effect of BMT increment on the gradually moving of $T_m$ to the low temperature as stated early. Also, the extremely huge $\varepsilon_{r,max}$ and narrow $\varepsilon_r$−$T$ curve of BMT0 demonstrate a typical ferroelectric-paraelectric phase transition of pure BZT. With increasing content of BMT, the $\varepsilon_{r,max}$ decreases significantly. The broad $\varepsilon_r$−$T$ peaks exhibited by the BZT−BMT ceramics with exception of BMT0 indicate the diffuse phase transition from ferroelectric to paraelectric phase. It can be said that the content of BMT has a significant effect on the maximum dielectric constant obtained as well as the diffuseness and broadening of the dielectric peaks of the BZT−BMT system.

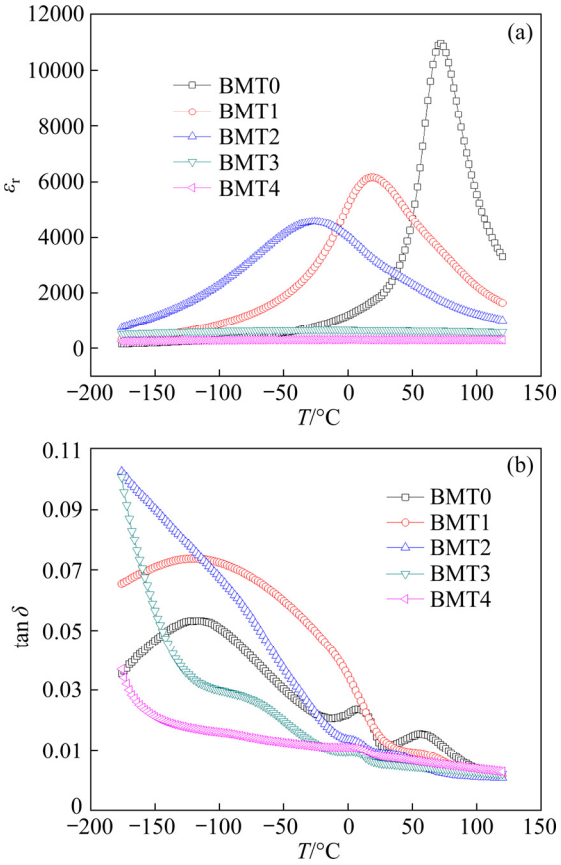


**Fig. 4** $\varepsilon_r$−$T$ (a) and tan $\delta$−$T$ (b) curves of BZT−BMT ceramics at 100 kHz

### 3.4 Diffuse phase transition

In diffuse phase transition systems, the dielectric maximum peaks are usually much broader and polarization keeps on for a short range of temperature above $T_m$. For solid solution systems, the above two characteristics are fulfilled by fluctuating the micro region composition around the mean composition to move the Curie point and at the same time making the ceramic uniformly mixed. This occurrence is used in almost all applicable Z5U and Y5V capacitors [33,34].

The diffuse phase transition is always characterized by a deviation from the Curie-Weiss law with respect to the Curie temperature. $1/\varepsilon_r$ starts to deviate from the Curie's law near $T_m$. Therefore, to study the phase transformation characteristics of BZT−BMT ceramics with temperature, the $T>T_m$ part is linearly fitted, as seen in Fig. 5.

Table 6 displays the specific parameters of various dielectric properties of BZT−BMT ceramics at 100 kHz, where $\Delta T_m$, $T_{cw}$, and $T_m$ represent the degree of deviation from the Curie-Weiss law, the temperature in the inverse of dielectric constant

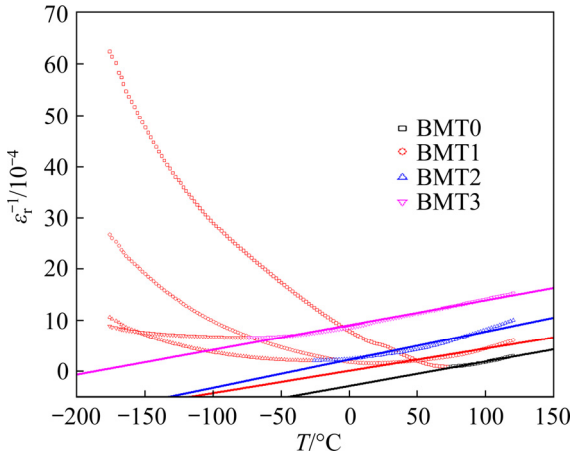


**Fig. 5** $1/\varepsilon_r$−$T$ curves of BZT−BMT ceramics at 100 kHz

**Table 6** Dielectric properties of BZT−BMT ceramics at 100 kHz

| Sample | $\varepsilon_{r,max}$ | $T_m$/°C | $T_{cw}$/°C | $\Delta T_m$/°C | $(\Delta\varepsilon_r/\varepsilon_r)$/% (−30 to 85 °C) |
|---|---|---|---|---|---|
| BMT0 | 10945 | 72 | 74.02 | 2.12 | (+473.37)−(−75.39) |
| BMT1 | 6159 | 18 | 75.74 | 57.74 | (+2.07)−(−64.80) |
| BMT2 | 4572 | −26 | 53.95 | 79.95 | (+52.60)−(−55.48) |
| BMT3 | 1430 | −68 | 17.64 | 85.64 | (+48.37)−(−35.93) |

$\Delta T_m=T_{cw}-T_m$

versus temperature graph (Fig. 5), and the dielectric maxima temperature, respectively [35]. The percentage of the permittivity variation ($\Delta\varepsilon_r/\varepsilon_r$) from −30 to 85 °C was calculated using the following equation:

$$\Delta\varepsilon_r/\varepsilon_r=\frac{\varepsilon_{r,T}-\varepsilon_{r,RT}}{\varepsilon_{r,RT}}\times100\% \quad (1)$$

where $\varepsilon_{r,T}$ is the relative permittivity at any other temperature, and $\varepsilon_{r,RT}$ is the relative permittivity at room temperature (25 °C).

$\Delta T_m$ showed a tendency to increase with increasing the BMT content in the composite system. Therefore, the degree of deviation from the Curie-Weiss law is heightened with the increase of BMT content.

It is known that the dielectric permittivity of a ferroelectric above the Curie temperature follows the modified Curie-Weiss law described by

$$\frac{1}{\varepsilon_r}-\frac{1}{\varepsilon_{r,max}}=\frac{(T-T_m)^\gamma}{C'} \quad (2)$$

where $\gamma$ and $C'$ are assumed to be constants [36].

To further describe the degree of diffuseness of the phase transition, the parameter $\gamma$ is obtained from the slope after linear fitting the data through $\ln(1/\varepsilon_r-1/\varepsilon_{r,max})-\ln(T-T_m)$. The $\gamma$ is known to convey information with regards to the characteristics of the phase transition. When $\gamma$=1, a normal Curie-Weiss law is obtained. At the other extreme ($\gamma$=2), a complete diffuse phase transition is described [35,37]. The $\gamma$ value increases from BMT0 to BMT3. It is noticeable that increasing the content of BMT affects the ferroelectric-paraelectric diffused phase transition behavior. The index $\gamma$ of pure BZT ceramic is 1.68987, indicating a normal ferroelectric with a diffused phase transition and the Sample BMT3 with $\gamma$= 2.00329 is a relaxor ferroelectric with a completely diffused-phase transition as exhibited in Fig. 6, which has some similarity to the report by TANG et al [38].

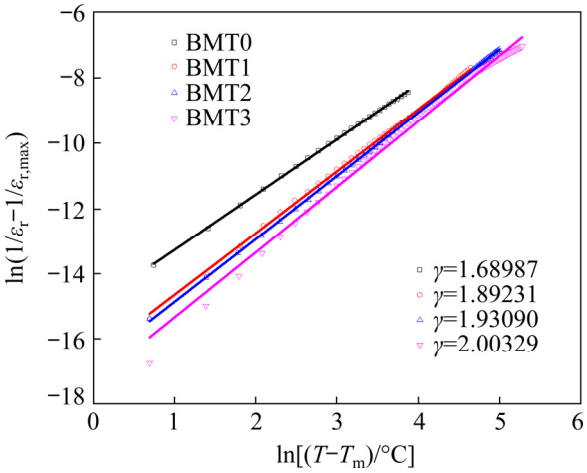


**Fig. 6** Plots of $\ln(1/\varepsilon_r-1/\varepsilon_{r,max})$ as function of $\ln(T-T_m)$ for BZT−BMT ceramics

In this analysis, it can be said that the inclusion of $Ba(Mg_{1/3}Ta_{2/3})O_3$ into BZT actuates and improves both the diffuseness and strength of the relaxation which is believed to be related to the arrangement of polar nano-regions due to variation of compositions [39]. The disorientation of the nano-regions hinders the strength of the ferroelectricity of material which is liable for the observed relaxor ferroelectric characteristics [40]. BMT3 showed the highest degree of diffusion, clearly indicating the broadness of the peaks. On the whole, the BZT−BMT system demonstrated a very good dielectric property at room temperature and can be implemented essentially to obtain Y5V

ceramic capacitors with better temperature stability. The capacitance of Y5V specification necessitates that capacitance falls within 22% or −82% from −30 to 85 °C [34].

### 3.5 Ferroelectric properties

The *P*−*E* hysteresis loops of the BZT−BMT ceramics under 20 kV at room temperature were measured, as shown in Fig. 7. With the increased content of BMT, the *P*−*E* hysteresis loops of ceramics gradually become thinner to straight lines with smaller gradients. The shape of the *P*−*E* hysteresis loop is in direct relation to the crystal structure of the material. It gets thinner as the temperature increases and becomes a single line above the Curie temperature when the material is no longer ferroelectric. Therefore, with the increase of the content of BMT at room temperature, the main crystal phase of the samples undergoes a transition from the ferroelectric phase to the paraelectric phase [41], which is not revealed by XRD analysis.

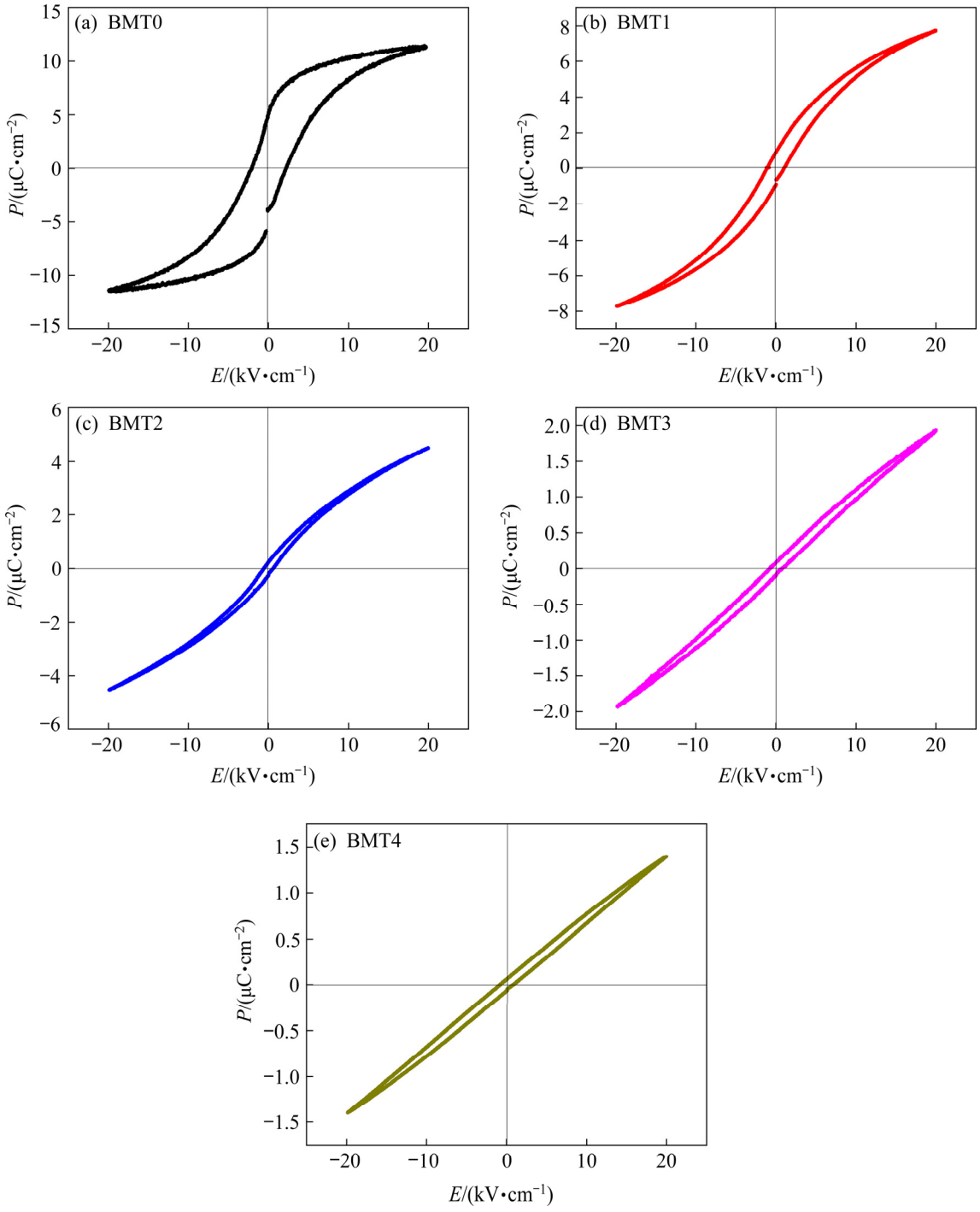


**Fig. 7** Hysteresis loop of BZT−BMT ceramics at room temperature

The remnant polarization ($P_r$) increases to the maximum 5.054 μC/cm$^2$ for the BMT0 sample as seen in Fig. 7(a) and then gradually decreases with the increase of $Ba(Mg_{1/3}Ta_{2/3})O_3$ content. The coercive field ($E_c$) of ceramics also decreases with increasing BMT content (Figs. 7(b)−(e)). The substitution of host *B*-site ions brings about elongation and weakening of the Ti—O bond, thus allowing a reverse in polarization to be achieved under a low coercive field. It is known that factors such as grain size, phase transition, ionic radius, and defect concentration strongly influence both $P_r$ and $E_c$ [42,43]. Therefore, this behavior can also be attributed to the drastic decrease in average grain size by increasing the content of BMT, contributing to the decrease in remnant polarization ($P_r$) [44] as summarized in Table 7.

**Table 7** Remnant polarization and coercive field of BZT−BMT ceramics at room temperature

| Sample | $2P_r$/(μC·cm$^{-2}$) | $2E_c$/(V·cm$^{-1}$) |
|---|---|---|
| BMT0 | 10.108 | 4.399 |
| BMT1 | 1.733 | 2.073 |
| BMT2 | 0.478 | 1.968 |
| BMT3 | 0.175 | 1.394 |
| BMT4 | 0.121 | 1.419 |

## 4 Conclusions

(1) The BZT−BMT ceramics prepared by the solid-stated method formed a perovskite solid solution with no impurity phases.

(2) The average grain sizes of BZT−BMT ceramics shrunk from 63.73 to 0.62 μm with increasing BMT content.

(3) Whilst increasing the BMT content, the dielectric maximum temperature shifted to lower temperatures. BMT introduced relaxor-like behaviors characterized by strong frequency dispersions and much defined diffuse phase transitions in the BZT system.

(4) A high relative permittivity of 6034 and a dielectric loss of 0.01399 prevailed for BMT1. And both the remnant polarization and the coercive field of the BZT−BMT ceramics reduced gradually with the increase of BMT content.

(5) BMT2 and BMT3 were identified as good candidates for Y5V ceramic capacitor application.

## Acknowledgments

This work is fully sponsored by the National Demonstration Center for Experimental Materials Science and Engineering Education (Jiangsu University of Science and Technology, China). And it is also funded by the Priority Academic Program Development (PAPD) of Jiangsu Higher Education Institutions, China.

## References

[1] SEBASTIAN M T, UBIC R, JANTUNEN H. Low-loss dielectric ceramic materials and their properties [J]. International Materials Reviews, 2015, 60: 392−412.

[2] PAN M J, RANDALL C A. A brief introduction to ceramic capacitors [J]. IEEE Electrical Insulation Magazine, 2010, 26: 44−50.

[3] VIJATOVIĆ M M, BOBIĆ J D, STOJANOVIĆ B D. History and challenges of barium titanate: Part I [J]. Science of Sintering, 2008, 40: 155−165.

[4] XU Qi, LIU Han-xing, ZHANG Lin, XIE Juan, HAO Hua, CAO Ming-he, LANAGAN M T. Structure and electrical properties of lead-free $Bi_{0.5}Na_{0.5}TiO_3$-based ceramics for energy-storage applications [J]. RSC Advances, 2016, 6: 59280−59291.

[5] DONG Xiao-yan, LI Xu, CHEN Hong-yun, SUN Cong-cong, SHI Jun-peng, PANG Fei-hong, ZHOU Huan-fu. Effective strategy to realise excellent energy storage performances in lead-free barium titanate-based relaxor ferroelectric [J]. Ceramics International, 2021 47: 6077−6083.

[6] CHANDRAKALA E, PRAVEEN J P, HAZRA B K, DAS D. Effect of sintering temperature on structural, dielectric, piezoelectric and ferroelectric properties of sol−gel derived BZT−BCT ceramics [J]. Ceramics International, 2016, 42: 4964−4977.

[7] SAITO Y, TAKAO H, TANI T, NONOYAMA T, TAKATORI K, HOMMA T, NAGAYA T, NAKAMURA M. Lead-free piezoceramics [J]. Nature, 2004, 432: 84−87.

[8] VIJATOVIĆ M M, BOBIĆ J D, STOJANOVIĆ B D. History and challenges of barium titanate: Part II [J]. Science of Sintering, 2008, 40: 235−244.

[9] RICHERSON D W, LEE W E. Modern ceramic engineering [M]. 4th ed. Florida: CRC Press, 2018.

[10] HONG K, LEE T H, SUH J M, YOON S H, JANG H W. Perspectives and challenges in multilayer ceramic capacitors for next generation electronics [J]. Journal of Materials Chemistry C, 2019, 7: 9782−9802.

[11] BIEGALSKI M D, QIAO L, GU Y J, MEHTA A, HE Q, TAKAMURA Y, BORISEVICH A, CHEN L Q. Impact of symmetry on the ferroelectric properties of $CaTiO_3$ thin films [J]. Applied Physics Letters, 2015, 106: 162904.

[12] RAMÍREZ M A, BUENO P R, LONGO E, VARELA J A. Conventional and microwave sintering of $CaCu_3Ti_4O_{12}$/$CaTiO_3$ ceramic composites: Non-ohmic and dielectric properties [J]. Journal of Physics D: Applied Physics, 2008, 41: 152004.

[13] ZHANG S J, LIM J B, LEE H J, XIA R, SHROUT T R.

$(K_{0.5}Na_{0.5})NbO_3$ based lead free piezoelectrics with expanded temperature usage range [C]//17th IEEE International Symposium on the Applications of Ferroelectrics. Santa Re, NM, USA: IEE, 2008: 1−2.

[14] WANG Ke, LI Jing-feng. (K,Na)$NbO_3$-based lead-free piezoceramics: Phase transition, sintering and property enhancement [J]. Journal of Advanced Ceramics, 2012, 1: 24−37.

[15] CHEN Xiao-ming, LIAO Yun-wen, MAO Li-jun, DENG Yi-lan, WANG Huai-ping, CHEN Qiang, XU Guang-liang. Microstructure and piezoelectric properties of Li-doped $Bi_{0.5}(Na_{0.825}K_{0.175})_{0.5}TiO_3$ piezoelectric ceramics [J]. Physica Status Solidi (a), 2009, 206: 1616−1619.

[16] IRIE H, MIYAYAMA M, KUDO T. Structure dependence of ferroelectric properties of bismuth layer-structured ferroelectric single crystals [J]. Journal of Applied Physics, 2001, 90: 4089−4094.

[17] KUMAR S, VARMA K B R. Dielectric relaxation in bismuth layer-structured $BaBi_4Ti_4O_{15}$ ferroelectric ceramics [J]. Current Applied Physics, 2011, 11: 203−210.

[18] ELBASSET A, ABDI F, LAMCHARFI T, SAYOURI S, ABARKAN M, ECHATOUI N S, AILLERIE M. Influence of Zr on structure and dielectric behavior of $BaTiO_3$ ceramics [J]. Indian Journal of Science and Technology, 2015, 8: 56574−56581.

[19] TAKAHASHI H, NUMAMOTO Y, TANI J J, TSUREKAWA S. Piezoelectric properties of $BaTiO_3$ ceramics with high performance fabricated by microwave sintering [J]. Japanese Journal of Applied Physics, 2006, 45(9B): 7405−7408.

[20] KARAKI T, YAN K, MIYAMOTO T, ADACHI M. Lead-free piezoelectric ceramics with large dielectric and piezoelectric constants manufactured from $BaTiO_3$ nano-powder [J]. Japanese Journal of Applied Physics, 2007, 46: L97−L98.

[21] HENNINGS D, SCHNELL A, SIMON G. Diffuse ferroelectric phase transitions in $Ba(Ti_{1-y}Zr_y)O_3$ ceramics [J]. Journal of the American Ceramic Society, 1982, 65: 539−544.

[22] NEIRMAN S M. The Curie point temperature of Ba $(Ti_{1-x}Zr_x)O_3$ solid solutions [J]. Journal of Materials Science, 1988, 23: 3973−3980.

[23] ZHAO Chun-lin, HUANG Yan-li, WU Jia-gang. Multifunctional barium titanate ceramics via chemical modification tuning phase structure [J]. InfoMat, 2020, 2: 1163−1190.

[24] COWLEY R A, GVASALIYA S N, LUSHNIKOV S G, ROESSLI B, ROTARU G M. Relaxing with relaxors: A review of relaxor ferroelectrics [J]. Advances in Physics, 2011, 60: 229−327.

[25] TIAN Yong-shang, GONG Yan-sheng, MENG Da-wei, LI Yuan-jian, KUANG Bo-ya. Dielectric dispersion, diffuse phase transition, and electrical properties of BCT-BZT ceramics sintered at a low-temperature [J]. Journal of Electronic Materials, 2015, 44: 2890−2897.

[26] KANTHA P, PISITPIPATHSIN N, PROMSAWAT M, PETNOI N, JIANSIRISOMBOON S, PENGPAT K, POJPRAPAI S. The effect of BZT doping on phase formation, dielectric and ferroelectric properties of BNLT ceramics [J]. Journal of Materials Science: Materials in Electronics, 2015, 26: 8456−8463.

[27] ZHONG Xin, ZHANG Chen, CHEN Fang-xu, TANG Zhu-ming, JIAN Gang. Dielectric properties and relaxor ferroelectric behavior of $(1-y)Ba(Zr_{0.1}Ti_{0.9})O_3-yBa(Zn_{1/3}Nb_{2/3})O_3$ ceramics [J]. Transactions of Nonferrous Metals Society of China, 2020, 30: 756−764.

[28] PENG Sen, XU Jian-ming. Microwave dielectric properties of $BaWO_4$-doped $Ba(Mg_{1/3}Nb_{2/3})O_3$ ceramics [J]. Journal of Materials Science: Materials in Electronics, 2020, 31: 22171−22178.

[29] CUI Xue-jiao, LIU Liang, LI Hao, LIU Fei, CHENG Li-jing, LIU Shao-jun. Influences of Mg and Mn doping on structure, B-site ordering and microwave dielectric properties of Ba $(Co_{1/3}Nb_{2/3})O_3$ ceramics [J]. Materials Research Express, 2020, 7: 016306.

[30] LIAN Fang, XU Li-hua, FU Zhi, CHEN Ning. Electronic structure calculations of $Ba(Mg_{1/3}Nb_{2/3})O_3$ and its dielectric properties analysis [J]. Key Engineering Materials, 2007, 280−283: 39−42.

[31] KE Shan-ming, FAN Hui-qing, HUANG Hai-tao, CHAN H L W, YU Shu-hui. Dielectric dispersion behavior of $Ba(Zr_xTi_{1-x})O_3$ solid solutions with a quasiferroelectric state [J]. Journal of Applied Physics, 2008, 104: 034108.

[32] ZHANG Chen, LING Zhi-xin, JIAN Gang, CHEN Fang-xu. Dielectric properties and point defect behavior of antimony oxide doped Ti deficient barium strontium titanate ceramics [J]. Transactions of Nonferrous Metals Society of China, 2017, 27: 2656−2662.

[33] HONG Jian-yu, LU Hong-yang. Polar nanoregions and dielectric properties of $BaTiO_3$-based $Y_5V$ multilayer ceramic capacitors [J]. Journal of the American Ceramic Society, 2014, 97: 2256−2263.

[34] ZHANG Xiao-hua, ZHANG Jie, ZHOU Yuan-yuan, XIE Zhen-kun, YUE Zhen-xing, LI Long-tu. Highly accelerated resistance degradation and thermally stimulated relaxation in $BaTiO_3$-based multilayer ceramic capacitors with $Y_5V$ specification [J]. Journal of Alloys and Compounds, 2016, 662: 308−314.

[35] THAKRE A, KUMAR A, LEE M Y, PATIL D R, KIM S H, RYU J. Artificially induced normal ferroelectric behaviour in aerosol deposited relaxor 65PMN−35PT thick films by interface engineering [J]. Journal of Materials Chemistry C, 2021, 9: 3403−3411.

[36] UCHINO K, NOMURA S. Critical exponents of the dielectric constants in diffused-phase-transition crystals [J]. Ferroelectrics, 1982, 44: 55−61.

[37] ZHANG Qiang, LI Zhen-rong, LI Fei, XU Zhuo. Structural and dielectric properties of Bi $(Mg_{1/2}Ti_{1/2})O_3-BaTiO_3$ lead-free ceramics [J]. Journal of the American Ceramic Society, 2011, 94: 4335−4339.

[38] TANG X G, CHEW K H, CHAN H L W. Diffuse phase transition and dielectric tunability of Ba $(Zr_yTi_{1-y})O_3$ relaxor ferroelectric ceramics [J]. Acta Materialia, 2004, 52: 5177−5183.

[39] VÖGLER M, NOVAK N, SCHADER F H, RÖDEL J. Temperature-dependent volume fraction of polar nanoregions in lead-free $(1-x)(Bi_{0.5}Na_{0.5})TiO_3-xBaTiO_3$ ceramics [J]. Physical Review B, 2017, 95: 024104.

[40] XIE L, LI Y L, YU R, CHENG Z Y, WEI X Y, YAO X, JIA C

L, URBAN K, BOKOV A A, YE Z G. Static and dynamic polar nanoregions in relaxor ferroelectric $Ba(Ti_{1-x}Sn_x)O_3$ system at high temperature [J]. Physical Review B, 2012, 85: 014118.

[41] SANGWAN K M, AHLAWAT N, KUNDU R S, RANI S, RANI S, AHLAWAT N, MURUGAVEL S. Improved dielectric and ferroelectric properties of Mn doped barium zirconium titanate (BZT) ceramics for energy storage applications [J]. Journal of Physics and Chemistry of Solids, 2018, 117: 158−166.

[42] CAI Wei, FU Chun-lin, LIN Ze-bin, DENG Xiao-ling. Vanadium doping effects on microstructure and dielectric properties of barium titanate ceramics [J]. Ceramics International, 2011, 37: 3643−3650.

[43] CHEN Jian, FU Chun-lin, CAI Wei, CHEN Gang, RAN S. Microstructures, dielectric and ferroelectric properties of $BaHf_xTi_{1-x}O_3$ ceramics [J]. Journal of Alloys and Compounds, 2012, 544: 82−86.

[44] CAI Wei, FU Chun-lin, GAO Jia-cheng, LIN Ze-bin, DENG Xiao-ling. Effect of hafnium on the microstructure, dielectric and ferroelectric properties of $Ba[Zr_{0.2}Ti_{0.8}]O_3$ ceramics [J]. Ceramics International, 2012, 38: 3367−3375.

# $(1-x)Ba(Zr_{0.1}Ti_{0.9})O_3-xBa(Mg_{1/3}Ta_{2/3})O_3$ 陶瓷的弛豫铁电及介电性能

Jesse Nii Okai AMU-DARKO[1,2]，张 晨[1]，Shahid HUSSAIN[2]，
Samuel Leumas OTOO[3]，Michael Freduah AGYEMANG[4]

1. 江苏科技大学 材料科学与工程学院， 镇江 212100；
2. 江苏大学 材料科学与工程学院， 镇江 212013；
3. 武汉理工大学 材料科学与工程学院，武汉 430070；
4. Department of Materials and Earth Sciences,
Technische Universität Darmstadt Alarich-Weiss-Straße 2, 64287 Darmstadt, Germany

**摘 要：**采用传统固相法在 1400 ℃在空气气氛中烧结 2 h 制备得到环境友好的$(1-x)Ba(Zr_{0.1}Ti_{0.9})O_3-xBa(Mg_{1/3}Ta_{2/3})O_3$ ($x$=0，0.02，0.04，0.06，0.08) 弛豫铁电陶瓷，借助 SEM 和 XRD 分别研究其表面形貌及晶体结构。同时研究 $Ba(Mg_{1/3}Ta_{2/3})O_3$ 对 $Ba(Zr_{0.1}Ti_{0.9})O_3$ 陶瓷相变及介电、铁电性能的影响。结果表明：$(1-x)Ba(Zr_{0.1}Ti_{0.9})O_3-xBa(Mg_{1/3}Ta_{2/3})O_3$(BZT−BMT)钙钛矿单相陶瓷的平均粒径随 $Ba(Mg_{1/3}Ta_{2/3})O_3$ (BMT)含量增大而减小。随着 $x$ 增大，陶瓷体系出现伴有弥散相变和频率色散的弛豫铁电行为。0.98BZT−0.02BMT 陶瓷具有良好的介电性能，在 100 kHz 下其室温相对介电常数及介电损耗分别为 6034 和 0.01399。随着 BMT 含量的增大，体系剩余极化强度及矫顽场均减小，表明室温下体系铁电相态向顺电相态的转变。

**关键词：**锆钛酸钡；钙钛矿；弛豫铁电体；介电性能；相变

**(Edited by Xiang-qun LI)**